JCB Article

Crystal structure of Sar1-GDP at 1.7 Å resolution and the role of the NH_2 terminus in ER export

Mingdong Huang,[1,2] Jacques T. Weissman,[1] Sophie Béraud-Dufour,[1] Peng Luan,[1] Chenqian Wang,[1] Wei Chen,[1] Meir Aridor,[1] Ian A. Wilson,[2,4] and William E. Balch[1,2,3]

[1]Department of Cell Biology, [2]Department of Molecular Biology, [3]The Institute of Childhood and Neglected Diseases, and [4]The Skaggs Institute for Chemical Biology, The Scripps Research Institute, La Jolla, CA 92130

The Sar1 GTPase is an essential component of COPII vesicle coats involved in export of cargo from the ER. We report the 1.7-Å structure of Sar1 and find that consistent with the sequence divergence of Sar1 from Arf family GTPases, Sar1 is structurally distinct. In particular, we show that the Sar1 NH_2 terminus contains two regions: an NH_2-terminal extension containing an evolutionary conserved hydrophobic motif that facilitates membrane recruitment and activation by the mammalian Sec12 guanine nucleotide exchange factor, and an α1′ amphipathic helix that contributes to interaction with the Sec23/24 complex that is responsible for cargo selection during ER export. We propose that the hydrophobic Sar1 NH_2-terminal activation/recruitment motif, in conjunction with the α1′ helix, mediates the initial steps in COPII coat assembly for export from the ER.

Introduction

The selective export of membrane-bound and soluble cargo from the ER is an evolutionarily conserved function that is central to cell development and proliferation. ER export is regulated by the Sar1 GTPase, a member of the Ras superfamily of small GTPases (Nakano and Muramatsu, 1989; Aridor and Balch, 1996; Barlowe, 1998; Springer et al., 1999). The GTPase activity of Sar1 functions as a molecular switch to control protein–protein and protein–lipid interactions that direct vesicle budding from the ER (Springer et al., 1999). Activation from the guanosine 5′-diphosphate (GDP)-* to the GTP-bound form of Sar1 involves the membrane-associated guanine nucleotide exchange factor (GEF) Sec12, first identified in yeast (Nakano et al., 1988; Barlowe et al., 1993; D'Enfert et al., 1991). A transmembrane homologue of yeast Sec12 has recently been identified in higher eukaryotes (Weissman et al., 2001). Activation of Sar1 by Sec12 in mammalian cells is coordinated with the selective recruitment of biosynthetic cargo and the COPII cytosolic coat complexes Sec23/24 and Sec13/31, leading to vesicle formation in both yeast and mammalian cells (Balch et al., 1994; Aridor et al., 1998; Kuehn et al., 1998; Springer et al., 1999). During or after fission of vesicles from the ER, GTP hydrolysis is stimulated by the recruited Sec23/24 GTPase-activating protein (GAP) complex to promote coat disassembly (Barlowe et al., 1994) and subsequent delivery of cargo to the Golgi complex (Palade, 1975).

The molecular and structural basis by which Sar1 coordinates COPII coat assembly and disassembly remains unknown. We now report the three-dimensional structure of the Sar1 GTPase in its GDP-bound form using x-ray crystallography. It has been assumed that Sar1 may have similar structural and biochemical features to its closest evolutionary relatives (~30% identity), members of the ADP-ribosylation factor (ARF) GTPase family, that function in recruitment of both clathrin and COPI vesicle coats (Wieland and Harter, 1999; Jackson and Casanova, 2000). However, we find that Sar1 has a number of structurally unique features that dictate its biological function. In particular, we illustrate that Sar1 is unlike all Ras superfamily GTPases that use either myristoyl or prenyl groups to direct membrane association and function, in that Sar1 lacks such modifications. Instead, Sar1 contains a unique nine-amino-acid NH_2-terminal extension. We find that this extension contains an evolutionarily

The online version of this article contains supplemental material.

Address correspondence to William Balch, Dept. of Cell Biology, IMM-11, The Scripps Research Institute, 10550 N. Torrey Pines Rd., La Jolla, CA 92037-1092. Tel.: (858) 784-2310. Fax: (858) 784-9706. E-mail: webalch@scripps.edu

M. Huang and J.T. Weissman contributed equally to this work.

Dr. Huang's present address is Division of Hemostasis and Thrombosis, Beth Israel Deaconess Medical Center, Harvard Medical School, RE-319, 330 Brookline Ave., Boston, MA 02215.

*Abbreviations used in this paper: GAP, GTPase-activating protein; GDP, guanosine 5′-diphosphate; GEF, guanine nucleotide exchange factor; MAD, multiwavelength anomalous diffraction; rmsd, root mean square deviation; STAR, Sar1–NH_2-terminal activation recruitment; VSV-G, vesicular stomatitis virus glycoprotein.

Key words: Sar1; ER; COPII; vesicle transport; Golgi

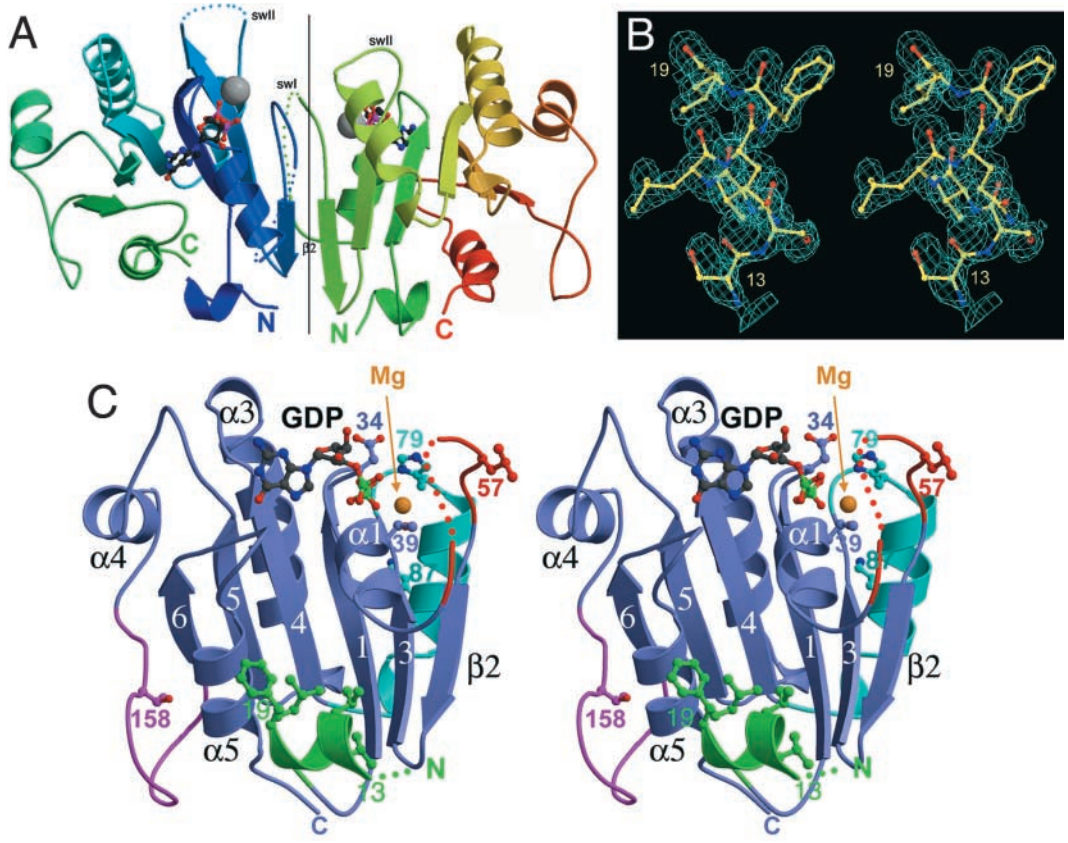

Figure 1. **Crystal structure of Sar1-GDP at 1.7 Å resolution.** (A) Ribbon representation of Sar1-GDP dimer (see supplemental Materials and methods, available at http://www.jcb.org/cgi/content/full/200106039/DC1). The unobserved regions in the electron density are represented by dotted lines. The polypeptide backbone representation was generated by Molscript (Kraulis, 1991) and Raster 3D (Merritt et al., 1997) and is colored blue to green from the NH_2 to COOH terminus for molecules A, and from green to red for molecule B. The noncrystallographic twofold axis between the monomers is indicated by a solid black line. The GDP is shown in stick figure representation, and the Mg ion as a large gray ball. Location of switch I (sw I) and switch II (sw II) regions are indicated. (B) Stereoview of the σ_A-weighted 2Fo-Fc omit electron density map, contoured at 2.0 σ, showing the Sar1 NH_2-terminal α1′ helix (residues 13–19). (C) Stereo Molscript (Kraulis, 1991) ribbon representation of Sar1-GDP structure at 1.7 Å. The secondary structure elements were assigned with reference to Arf1 and Ras GTPases. The NH_2-terminal helix (α1′) is in green and the Ω loop (residues 156–171) unique to Sar1 is shown in magenta. The location of the Mg ion is shown as a yellow sphere. The bound GDP is shown in a ball and stick figure representation; gray, carbons; red, oxygens; blue, nitrogens; and green, phosphate. Switch I and II regions involved in guanine nucleotide exchange and hydrolysis are shown in red and cyan, respectively. The unobserved residues in the electron density maps are represented by dotted lines. Residues reported in the Results that have been mutagenized as described (Kuge et al., 1994; Aridor et al., 1995) are indicated.

conserved cluster of bulky hydrophobic amino acids, referred to as the Sar1–NH_2-terminal activation recruitment (STAR) motif. We show that the STAR motif mediates the recruitment of Sar1 to ER membranes and facilitates its interaction with the mammalian Sec12 GEF leading to activation. In addition, we show that an NH_2-terminal amphipathic α1′ helix facilitates functional interaction with the Sec23/24 GAP complex. Our results provide a structure-based mechanism for understanding the first step in Sar1 function that coordinates cargo selection with the recruitment of the COPII coat to initiate ER export.

Results

Structure determination

His_6-tagged full-length hamster Sar1 was expressed and purified from *Escherichia coli* (Rowe et al., 1996), but failed to crystallize due to formation of higher order oligomers. Therefore, we generated an NH_2-terminal Δ9-Sar1A mutant that was monodispersed in solution. The protein had a native apparent molecular mass of 43.6 kD corresponding to a dimer that yielded diffraction quality crystals (unpublished data). The three-dimensional structure of Δ9-Sar1 in the GDP-bound form (abbreviated as Sar1-GDP) was determined by the multiwavelength anomalous diffraction (MAD) method using data from its selenomethionine derivative to 2.0 Å resolution. Sar1 is sufficiently different than Arf GTPases, such that obtaining a structure based on homology modeling with Arf was difficult.

The structure was refined against native Sar1-GDP data to 1.7 Å to R_{cryst} and R_{free} values of 22.2 and 24.2%, respectively (Tables I and II; Fig. 1). Overall, the structure was well defined with an average B value of 21.4 $Å^2$, and an estimated overall coordinate error of 0.22 Å. Consistent with dynamic light scattering measurements in aqueous solution, two Sar1-GDP molecules (A and B) formed a dimer in the crystallographic asymmetric unit with the noncrystallographic twofold axis running between and parallel to the β2

Table I. **Statistics of x-ray data collection and structural refinement for Sar1-GDP crystals**

		MAD of SeMET derivative		
Crystal	**Native**	**Remote**	**Inflection Point**	**Peak**
Wavelength (Å)	1.08	1.08	0.9796	0.9795
Synch. Source (SSRL)	BL7-1	BL9-2	BL9-2	BL9-2
Resolution (Å)	1.70	2.00	1.79	1.90
R_{merge}[a]	0.050 (0.26)[b]	0.071 (0.33)	0.074 (0.64)	0.095 (0.79)
I/σ	24.5 (5.4)[b]	19.7 (5.0)	26.4 (3.7)	20.0 (2.6)
R_{cullis}			0.45	0.68
Refined f′,f′′ (iso/ano)			−24.1/4.8	−17/3.5
Rms F_h/E for acentric reflections[c]				
dispersive			3.8	2.4
anomalous			1.7	1.4
Overall FOM for acentric reflections			0.47 (0.26)	

[a]$R_{merge}(I) = \Sigma|I(i) - <I(h)>|/\Sigma I(i)$, where $I(i)$ is the ith observation of the intensity of the *hkl* reflection and $<I>$ is the mean intensity from multiple measurements of the *hkl* reflection.
[b]Numbers in the parentheses are for the last resolution shell (1.81 − 1.70 Å for the native date set).
[c]Rms F_h/E represents phasing power; rms, root mean square; F_h, heavy-atom structure factor amplitude; E, residual lack of closure error.

strands (Fig. 1 A). The root mean square deviation (rmsd) of 0.56 Å for 166 equivalent Cα atoms confirmed highly similar core structures. However, the dimerization through the parallel pairing of segments of their respective β2 strands (molecule A, 61-SEELTI-66; molecule B, 60-TSEELT-65) is slightly asymmetric and is mediated by five main chain hydrogen bonds and three side chain hydrogen bonds (63E[molecule A]–46K[molecule B]; 46K[A]–61S[B]; and 60T[A]–81Q[B]). This dimerization differs from Arf1-GDP, which forms a symmetric dimer through its unique β2ε strands (Amor et al., 1994; Greasley et al., 1995).

The structural core of Sar1

Sar1 (Fig. 1 C) has a structural core of six central β strands (5 parallel, 1 antiparallel [β2]; in order: 6, 5, 4, 1, 3, 2) in a relatively flat β sheet that is sandwiched between three α helices on either side. This motif forms a typical Ras superfamily guanine nucleotide-binding pocket (Schweins and Wittinghofer, 1994), with the relatively flat β sheet being more characteristic, but different than that of the Arf family GTPases (Amor et al., 1994; Greasley et al., 1995) (Fig. S1, available at http://www.jcb.org/cgi/content/full/200106039/DC1). The nucleotide (GDP) is partially buried in the binding pocket with the ribose ring more exposed than the phosphate and purine moieties (Fig. 1 C). The hydrophobic face of the purine ring is sandwiched by the aliphatic side chains of Leu181 and Lys135.

The GDP-binding site includes residues found in all of the highly conserved binding motifs diagnostic of GTPases. Thr39 is found in the conserved GxxxxGKT[39] motif, and is essential for Sar1 function. In particular, the Sar1 dominant negative mutant Sar1[T39N] is a potent inhibitor of COPII vesicle formation (Kuge et al., 1994; Aridor and Balch, 1996; Rowe et al., 1996). Other Ras superfamily GTPases with mutations in the homologous residue are restricted to their GDP-bound form and inhibit their respective GEF activity. We have shown that Sar1[T39N] inhibits wild-type Sar1 function in vivo and in vitro by interfering with its interaction with mammalian Sec12 (mSec12), the ER-associated GEF that is required for Sar1 activation and COPII vesicle formation (Weissman et al., 2001). Moreover, Asp34 within the GxD[34]xxGK(S/T) guanine nucleotide binding motif is an invariant residue in the Sar1 family that aligns with Gly12 of Ras. Mutation of Gly12 in Ras greatly reduces the intrinsic GTP hydrolysis rate leading to prolonged activation and cell transformation (Wittinghofer and Pai,

Table II. **Statistics of model refinement against native data set**

Space group and cell parameters	$P2_1$, a =53.37 Å, b = 61.69 Å, c = 71.14Å, b =107.5°
Resolution	15-1.7Å
Total reflections	46,597 (6717)[b]
Protein nonhydrogen atoms	2882
Solvent molecules (H_2O, SO_4)	297, 5
R_{cryst}[a]	0.22 (0.26)
R_{free}[a]	0.24 (0.28)
Residues in the model	A chain: 13–48 55–78 83–198; B chain: 13–49 55–198
Overall average B-value (Å2)	21
Waters	30
Protein	20
Sulphates	29
Rmsd of bond lengths/angles	0.006Å/1.6°
Estimated coordinate error (16)	0.22Å

[a]$R_{cryst}(F) = \Sigma_h||F_{obs}(h)| - |F_{calc}(h)||/\Sigma_h|F_{obs}(h)|$, where $|F_{obs}(h)|$ and $|F_{calc}(h)|$ are the observed and calculated structure factor amplitudes for the *hkl* reflection. R_{free} is calculated over reflections in the test set of 1857 reflections (4%) not included in atomic refinement.
[b]Numbers in parentheses are for the last resolution shell (1.81–1.7 Å).

1991). In contrast, mutation of Asp34 to Gly in yeast Sar1 interferes with GTP-loading in vitro and destroys its ability to function in vesicle budding (Saito et al., 1998).

The Mg ion involved in guanine nucleotide binding in molecule B of Sar1-GDP shows octahedral coordination geometry typical for small GTPases. It is coordinated by an oxygen atom of the β phosphate of GDP, the hydroxyl oxygen of a conserved Thr residue (residue 39 in Sar1-GDP) of the phosphate-binding GxxxxGKS/T motif (Fig. 1 C) (corresponding to residues 10–17 of Ras where x is a variable residue) (Wittinghofer and Pai, 1991), and four water molecules with Mg-O bond distances of 2.23 Å, 2.19 Å, 2.31 Å, 2.31 Å, 2.30 Å, and 2.32 Å, respectively. Two of the water molecules (w22 and w5) are further hydrogen bonded to Asp75 that belongs to the highly conserved DxxG motif in the switch II region.

Organization of switch regions in Sar1-GDP

Ras superfamily GTPases contain two switch regions (I and II) that are involved in interaction with effectors that promote guanine nucleotide exchange and hydrolysis (Vetter and Wittinghofer, 2001). In Sar1, both switch I and II loops are proximal to the dimer interface (Fig. 1 A). Based on structural alignment with other Ras superfamily GTPases, the switch regions in Sar1 encompass residues 48–59 (switch I) and 78–94 (switch II). The Sar1 switch I residues (55–59) in both molecules are close to the guanine nucleotide, consistent with the role of the switch I loop in mediating indirect interaction between effector molecules and guanine nucleotide. In contrast, a segment of the switch I residues in Arf1-GDP form a novel β2ϵ strand that is distant from the guanine nucleotide binding site (Amor et al., 1994; Greasley et al., 1995). Consistent with the role of the two switch regions in mediating Sar1 function, mutation of specific residues in either switch I (Leu57) (Fig. 1 C) or II (Lys87) (Fig. 1 C) interferes with COPII vesicle budding and ER export in vivo and in vitro (unpublished data). The homologous mutations in ARF1 disrupt the interaction of ARF1 with the ARF1-specific GEF ARNO (Beraud-Dufour et al., 1998, 1999).

Residues 10–12, 49–54, and 79–81 of molecule A, and residues 10–12 and 50–54 of molecule B that include segments in the switch regions, lack electron density and were omitted from final model of Sar1 (Fig. 1, A and C). A similar lack of density in the switch regions of other GDP-bound forms of Ras superfamily members is frequently observed and reflects the extensive conformational changes that accompany interaction with effectors and GDP/GTP exchange. Whereas switch II (79–82) is well ordered in molecule B, the disorder in molecule A is partly due to the loss of a hydrogen bond between His79 and Asp34, which results in Asp34 swinging away from His79. His79 in Sar1 corresponds to Gln61 in Ras-GTP (Wittinghofer and Pai, 1991) and Gln71 in Arf1-GTP (Amor et al., 1994; Greasley et al., 1995), both of which are important for the hydrolysis of GTP. Consistent with this role, the Sarl[H79G] mutant is a potent inhibitor of ER to Golgi transport that prevents the disassembly of COPII vesicle coats as a consequence of its reduced rate of Sec23/24 GAP-stimulated hydrolysis (Rowe et al., 1996; Aridor et al., 1998, 1999).

Distinctive structural features of Sar1

Sar1 has a number of distinctive features that separate it from Ras superfamily GTPases including Arf (Fig. S1, available at http://www.jcb.org/cgi/content/full/200106039/DC1). Sar1-GDP lacks the extended COOH terminus found in Ras, Rho/Rac/Cdc42, and Rab GTPases. Instead, the COOH-terminal residues of Sar1-GDP are highly ordered, as in Arf1 and Arf6 (Amor et al., 1994; Greasley et al., 1995; Menetrey et al., 2000), and form an amphipathic helix (α5; residues 187–197) that covers the hydrophobic core of the central β sheet (Fig. 1, A and C). Other features differentiate Sar1 from Arf1. First, as indicated above, Sar1-GDP lacks the extra β strand (β2ϵ) found in Arf1 (Amor et al., 1994; Greasley et al., 1995) and Arf6 (Menetrey et al., 2000), which is adjacent to the β2 strand in the switch I region. The β2ϵ strand plays a critical role in transition from the GDP- to the GTP-bound state after interaction with Arf-specific GEFs (Antonny et al., 1997; Paris et al., 1997; Beraud-Dufour et al., 1999).

A second unique structural feature of Sar1 not observed in Arf GTPases or other Ras superfamily members is a novel insert encompassing residues 156–171, which are quite variable in sequence among evolutionarily distant members of the Sar1 family. These residues form a long surface-exposed loop (denoted as the Ω loop, as their NH_2 and COOH termini are adjacent to each other) connecting helix α4 and strand β6 (Fig. 1 C). The insert loop has a relatively high B value, 36 $Å^2$ as compared with the overall value of 21 $Å^2$. As β sheet proteins have a tendency to associate with other β sheet proteins through the pairing of their edge β strands, the high B value and the fact that the Sar1 Ω loop is located at the edge of the core β sheet suggests a potential functional role in regulating Sar1 interactions with other components of the COPII machinery. To test this possibility, we mutated the highly conserved Thr158 to Ala and analyzed its ability to support export of vesicular stomatitis virus glycoprotein (VSV-G) from the ER using an assay that reconstitutes COPII vesicle budding from ER microsomes in vitro (Rowe et al., 1996). Here, VSV-G–containing ER microsomes are incubated in the presence of Sar1(wild type and mutant) and purified Sec23/24 and Sec13/31 components, and the amount of VSV-G cargo recovered in the COPII vesicle fraction is quantitated. Consistent with the importance of this region in Sar1 function, we observed a complete loss activity with the Sar1[T158A] mutant (Fig. 2 A).

Sar1 contains an NH_2-terminal α1′ helix domain that facilitates interaction with the Sec23/24 GAP complex

The NH_2-terminal residues (15-VLNFL-19) of Sar1-GDP form an amphipathic helix (α1′) (Fig. 1 C, green). Arf1 GTPases also contain an NH_2-terminal α1′ helix (Amor et al., 1994; Greasley et al., 1995) that is essential for function, is believed to facilitate binding of Arf1 to the lipid bilayer (Antonny et al., 1997; Beraud-Dufour et al., 1999), and is essential for interaction with phospholipase D (Jones et al., 1999). However, the orientation of the Sar1 α1′ helix is very different than that of Arf1. Whereas the NH_2-terminal helices of Arf1-GDP and Arf6-GDP run parallel to the β strands of the central β sheet (Amor et al., 1994; Greasley et al., 1995; Menetrey et al., 2000), the Sar1-GDP NH_2-ter-

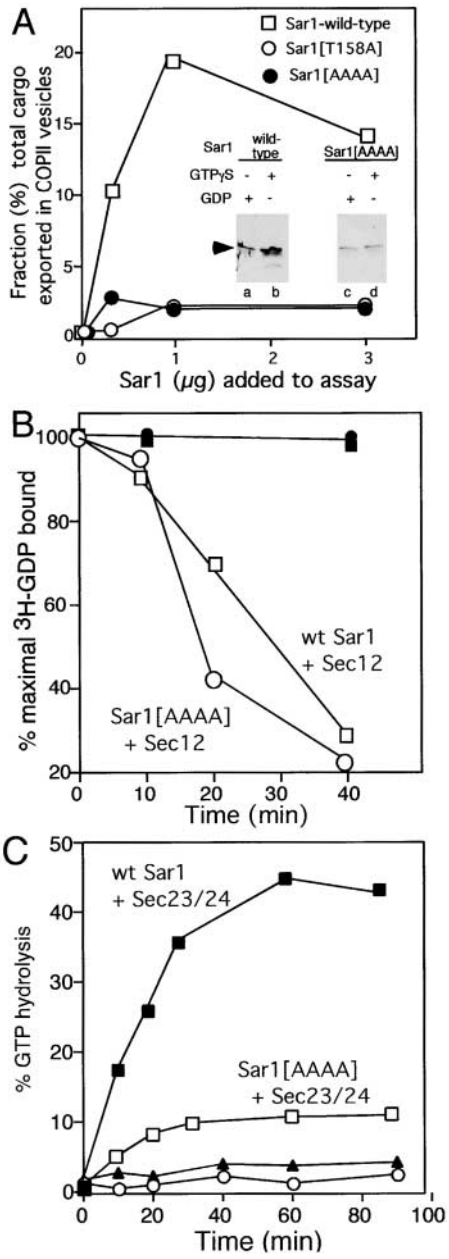

Figure 2. **The α1′ helix is critical for recognizing the Sec23/24 GAP complex.** (A) ER microsomes and purified, recombinant Sar1 wild-type and mutant proteins were prepared as described (Rowe and Balch, 1995). COPII vesicle budding assays were performed in the presence of purified Sec13/31 and Sec23/24 as described (Rowe et al., 1996; Aridor et al., 1998). (Inset) Microsomes were incubated for 10 min at 32°C in the presence of either 1 μg Sar1, 1 μg Sar1[AAAA], 100 μM GDP, or GTPγS as indicated. Microsomes were then pelleted and Sar1 recovered in the pellet quantitated using immunoblotting. (B) Sec12 mediated exchange was measured by preloading 1 μg of Sar1 with [^{3}H]-GDP and incubating in the presence of 1 mM cold GTP and the absence or presence of mammalian Sec12 protein (2 μg) (Weissman et al., 2001), and the amount of [^{3}H]-GDP remaining bound to Sar1 quantitated as described (Nuoffer et al., 1994). Closed circles and squares correspond to incubations lacking mSec12 in the presence of Sar1[AAAA] or wild-type Sar1, respectively. (C) Wild-type Sar1 (■, ▲) or Sar1[AAAA] (□, ○) were incubated alone (▲, ○) or with Sec23/24 (■, □) as indicated in the presence of α[^{32}P]GTP for various times. Sec23/24 incubated in the absence of Sar1 is shown by triangles. The amount of radiolabeled GDP and GTP were quantitated as described (Aridor et al., 1998).

minal helix is oriented perpendicular to the β sheet (Fig. 1 C). The NH_2-terminal helix is not found in other Ras superfamily GTPases, although a very short helix linked to an extended NH_2-terminal loop is found in the GDP structure of Arl3, an Arf-like GTPase of unknown function (Hillig et al., 2000).

To explore the potential role of the α1′-helix in Sar1 function, we generated a mutant in which the hydrophobic residues Val 15, Leu 16, Phe 18, and Leu 19 that principally contribute to packing of the α1′ helix to the hydrophobic core (Fig. 1 C), were mutated to Ala (Sar1[AAAA]). We first tested the ability of the mutant to support export of VSV-G from the ER into COPII vesicles in vitro (Rowe et al., 1996). Compared with wild-type Sar1 which supports efficient export from the ER, Sar1[AAAA] lost all activity (Fig. 2 A). Loss of activity was not due to misfolding of the core fold of Sar1, because the [AAAA] substitution had no effect on nucleotide binding (Fig. S2 A, available at http://www.jcb.org/cgi/content/full/200106039/DC1). Thus, the NH_2-terminal α1′ helix is essential for Sar1 function.

We next examined whether the Sar1[AAAA] mutant could be stably recruited to ER microsomes after activation by the nonhydrolyzable analogue of GTP, GTPγS. Whereas wild-type Sar1 was efficiently recruited to the ER after activation with GTPγS (Fig. 2 A, inset, compare a with b) as observed previously (Aridor et al., 1995), in the presence of GTPγS, the Sar1[AAAA] mutant failed to be recruited over levels observed in the GDP control (Fig. 2 A, inset, compare c with d). Thus, stable membrane recruitment to the ER membrane is sensitive to mutation of the α1′ helix.

Given the importance of the membrane-associated mammalian mSec12 GEF for Sar1 activation leading to COPII vesicle formation in vitro (Weissman et al., 2001), we examined the effect of the [AAAA] substitution on interaction of Sar1 with purified mSec12 GEF in the presence of detergent. Exchange was measured by preloading Sar1 with [^{3}H]-GDP and incubating in the presence of 1 mM cold GTP in the absence or presence of mSec12 (Weissman et al., 2001). mSec12 promoted efficient nucleotide exchange on wild-type Sar1 (Fig. 2 B). Moreover, the Sar1[AAAA] mutant had a comparable rate of mSec12-stimulated exchange. Because the mutation of the α1′ helix did not prevent interaction with mSec12, the inability of Sar1 to be activated by ER-associated mSec12 is not the explanation for its inability to support COPII vesicle budding in vitro.

The next step in COPII coat assembly from mammalian ER microsomes following activation of Sar1 is the recruitment of the cytosolic Sec23/24 coat complex to form detergent-resistant, prebudding complexes (Aridor et al., 1998). Therefore, we examined whether the α1′ helix was required for interaction with Sec23/24. As the Sec23/24 complex is a Sar1-specific GAP (Hicke and Schekman, 1989; Yoshihisa et al., 1993; Aridor et al., 1998), direct interaction between these proteins can be determined by examining the ability of purified mammalian Sec23/24 to accelerate GTP hydrolysis of activated Sar1 (Aridor et al., 1998). Wild-type Sar1 or the Sar1[AAAA] mutant were incubated the presence of purified Sec23/24 GAP and α[^{32}P]GTP, and the amount of radiolabeled GDP formed determined (Aridor et al., 1998). Whereas Sec23/24 promoted rapid GTP hydrolysis of wild-

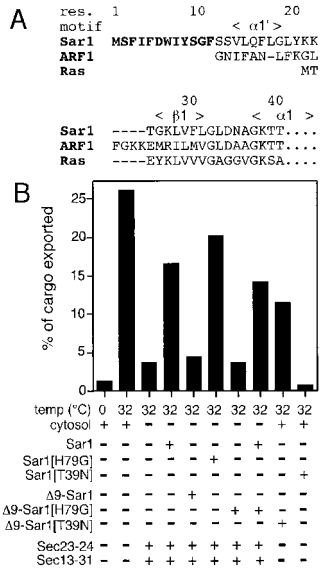

Figure 3. **Sar1 NH_2 terminus is required for function in vitro.** (A) Alignment of NH_2-terminal regions of representative Ras superfamily GTPases showing the unique NH_2-terminal extension found in Sar1. The α1′ helix indicated is that of Sar1. The Arf1 α1′ helix contains nine residues beginning at the NH_2-terminal Gly (Amor et al., 1994; Greasley et al., 1995). (B) ER microsomes were incubated in the presence of ATP, GTP, and cytosol or purified COPII components Sec23/24 and Sec13/31 for 30 min at 32°C, and then the amount of cargo released into the COPII vesicles was determined as described (Rowe et al., 1996). The (+) or (−) indicates the presence or absence of the various indicated components in the reaction mixture. The results are typical of three independent experiments.

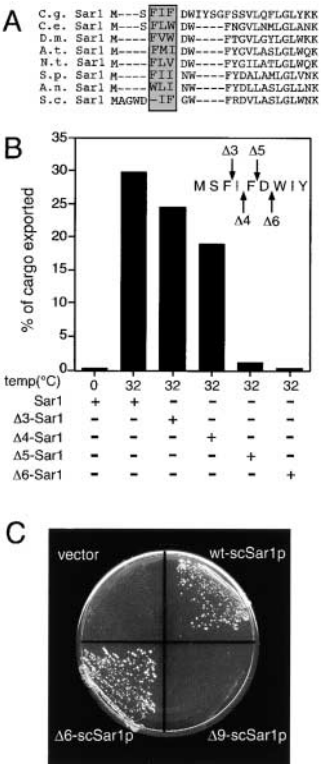

Figure 4. **The NH_2 terminus of Sar1 is evolutionarily conserved and essential for function.** (A) Sequence alignment of the NH_2-terminal residues of Sar1 GTPases (C.g., *Cricetulus griseus* [Chinese hamster]; C.e., *Caenorhabditis elegans*; D.m., *Drosophila melanogaster*; A.t., *Arabidopsis thalia*; N.t., *Nicotiana tabacum*; S.p., *Schizosaccharomyces pombe*; A.n., *Aspergillus niger*; and S.c., *Saccharomyces cerevisiae*). (B) ER microsomes were incubated in the presence of ATP, GTP, and purified COPII components for 30 min at 32°C, and then the amount of cargo released into the COPII vesicles was determined as described (Rowe et al., 1996). The (+) or (−) indicates the presence or absence of the various indicated components in the reaction mixture. The results are typical of three independent experiments. (C) Plasmids (CEN *LEU2*) containing control vector, wild-type *scSAR1*, *Δ6-scsar1*, or *Δ9-scsar1* were used to transform a *sar1Δ::HIS3* strain containing a CEN *URA3 scSAR1* plasmid as the sole source of wild-type scSar1p. Transformed strains were streaked to 5-fluoroorotic acid (5FOA) plates to select for loss of the *URA3 scSAR1* plasmid, leaving the mutant *scsar1* gene as the only source of Sar1p.

type Sar1, the Sar1[AAAA] mutant showed a markedly reduced rate and extent of Sec23/24 promoted GTP hydrolysis (Fig. 2 C). These results suggest that the failure of the Sar1[AAAA] mutant to be stably recruited to ER membranes (Fig. 2 A) to form COPII prebudding complexes may be related to its inability to interact with Sec23/24. This interpretation is consistent with previous results in which stable recruitment of activated Sar1 to ER membranes requires Sec23/24, which is essential to form detergent resistant prebudding complexes (Aridor et al., 1998). Thus, the α1′ helix functions to facilitate coat assembly on ER membranes.

An NH_2-terminal extension appended to the α1′ helix of Sar1 is required for function in vitro and in vivo

The COOH-terminal extensions found in Ras, Rho/Rac/Cdc42, and Rab-like GTPases contain prenyl-lipid modifications promoting membrane association (Seabra, 1998). In contrast, Arf family members contain a myristoyl modification attached to the Gly residue found at the NH_2 terminus of the α1′ helix (Kahn et al., 1988) (Fig. 3 A). These lipid modifications are essential for both membrane association and function.

Curiously, Sar1 lacks any known lipid modifications at either termini (unpublished data). However, appended to the NH_2 terminus of Sar1 is a unique extension not found in Arf family or other Ras superfamily members (Fig. 3 A). By analogy to the proposed role of the myristoyl group in Arf1 for bilayer association (Antonny et al., 1997; Beraud-Dufour et al., 1999), one possibility is that the NH_2-terminal extension of Sar1 contains information necessary for its binding to ER membranes to initiate COPII vesicle formation. Indeed, whereas wild-type Sar1 or the GTPase-defective mutant Sar1[H79G] support efficient COPII vesicle formation in vitro, a deletion mutant lacking residues 2–9 (Δ9-Sar1) or a Δ9-Sar1[H79G] double mutant (a mutant containing both the Δ9 truncation and the H79G substitution), were unable to support COPII vesicle budding in vitro (Fig. 3 B). Moreover, whereas ER vesicle formation in the presence of crude cytosol (which contains all three COPII components) can be blocked with the dominant negative GDP-restricted form of Sar1, Sar1[T39N] (Kuge et al., 1994; Aridor et al., 1995, 1998; Weissman et al., 2001), the double mutant, Δ9-Sar1[T39N] (a mutant containing both the Δ9 truncation and the T39N substitution), did not block vesicle formation (Fig. 3 B). A similar result was observed in vivo where the ability of the transiently expressed Sar1[T39N] to

block ER to Golgi transport was lost in the Δ9-Sar1[T39N] double mutant (unpublished data). Because Sar1[T39N] is an inhibitor of the Sar1-specific GEF (Weissman et al., 2001), we conclude that the NH_2-terminal extension participates in the initial events of COPII vesicle budding related to Sar1 recruitment and/or activation.

A hydrophobic patch within the NH_2 terminus is critical for ER export

Given the importance of the NH_2-terminal region in mammalian Sar1 function (Fig. 3 B), we examined whether the extension was found in evolutionarily divergent Sar1 GTPases. Remarkably, sequence alignment of divergent members of the Sar1 family illustrated that they not only contained an NH_2-terminal extension, but the alignment revealed a highly conserved bulky hydrophobic patch (Fig. 4 A). Therefore, to accurately define the region(s) of importance in the Sar1 NH_2 terminus in function, we characterized the activities of more limited NH_2-terminal truncations on VSV-G export into COPII vesicles in vitro (Fig. 4 B). Whereas deletion of amino acids 1–3 or 1–4 (Δ3, Δ4-Sar1) only weakly interfered with vesicle budding, strikingly, deletion beyond residues 5 (Δ5-Sar1) potently blocked vesicle formation. Thus, the hydrophobic patch appears to contribute significantly to COPII vesicle budding.

To determine whether the patch was also required for function in lower eukaryotes, we made deletions in the *Saccharomyces cervisiae* homologue of Sar1 (scSar1p) based on the sequence alignment of Sar1 homologs (Fig. 4 A). We focused on only two deletion mutants: Δ9-scSar1p corresponding to the mammalian Δ9-Sar1 truncation that lacked activity (Fig. 4 B), and Δ6-scSar1p corresponding to the mammalian Δ4-Sar1 mutant that retained significant activity (Fig. 4 B). When we introduced these two yeast constructs into a strain that lacks the Sar1 gene (*ΔSar1*), complementation was observed with Δ6-scSar1p, but not with the Δ9-scSar1p (Fig. 4 C). Thus, in agreement with the important role of the hydrophobic patch in ER export in vivo and in vitro in mammalian cells, the short sequence of bulky hydrophobic residues defines an evolutionarily conserved function.

The hydrophobic patch serves a motif for Sar1 function

The above experiments suggest that either the overall length of the NH_2 terminus is critical for Sar1 activity, or that the short, evolutionarily conserved patch encompassing several bulky hydrophobic residues is important for function (Fig. 4). To disrupt function of this patch, we chose a hydrophilic Asp residue to replace Phe 5 as deletion of 4 residues had little effect on Sar1 function, whereas deletion of 5 residues led to striking loss of function (Fig. 4 B). Strikingly, when we tested the ability of the Sar1[F5D] mutant to support budding in vitro, the mutant was unable to reconstitute COPII vesicle formation (Fig. 5 A). Moreover, it did not interfere with vesicle formation in the presence of cytosol-containing wild-type Sar1, demonstrating that the [F5D] mutant was not dominant negative (Fig. 5 A) like the [T39N] or [H79G] mutants. In addition, while Sar1[T39N] showed dominant negative activity in preventing vesicle budding in vitro (Fig. 5 A), the Sar1[T39N][F5D] double mutant lost

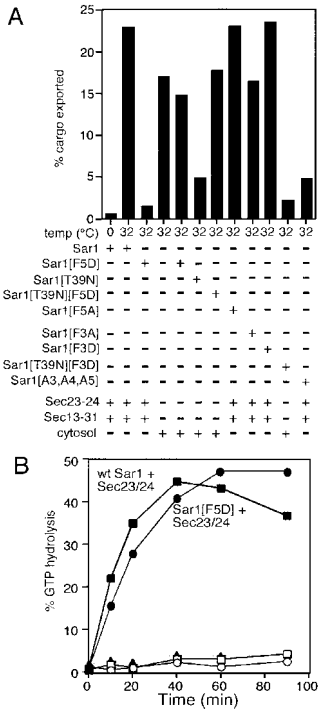

Figure 5. **The hydrophobic patch at the NH_2 terminus of Sar1 is essential for recognition of Sec23/24.** (A) ER microsomes were incubated in the presence of ATP, GTP, and rat liver cytosol or purified COPII components for 30 min at 32°C, and then the amount of cargo released into the COPII vesicles was determined as described (Rowe et al., 1996). The typical results of three independent experiments are shown. (B) Wild-type Sar1 (□, ■) or Sar1[F5D] (○, ●) were incubated alone (□, ○) or with Sec23/24 (■, ●, ▲) as indicated in the presence of $\alpha[^{32}P]$GTP for various times. Sec23/24 incubated in the absence of Sar1 is shown by triangles. The amount of radiolabeled GDP and GTP were quantitated as described (Aridor et al., 1998) (see supplemental Materials and methods, available at http://www.jcb.org/cgi/content/full/200106039/DC1).

its ability to function as a dominant negative inhibitor in vitro (Fig. 5 A) and in vivo (unpublished data). This result raises the possibility that the [F5D] substitution may uncouple the ability of the Sar1[T39N] mutant to interact with its specific ER-localized exchange factor mSec12 (Weissman et al., 2001).

In contrast to the [F5D] substitution, mutation of Phe 5 to Ala ([F5A]) had no effect on the wild-type activity of Sar1 to support vesicle budding in vitro (Fig. 5 A), or on the ability of the Sar1[T39N] mutant to inhibit ER to Golgi transport in vitro (Fig. 5 A) and in vivo (unpublished data). Thus, when mutated to Ala, loss of Phe5 function can be compensated by adjacent bulky hydrophobic residues suggesting that Phe3 and Ile4 may contribute to the formation of a general hydrophobic patch that promotes association with the lipid bilayer. Consistent with this possibly, a triple AAA substitution for residues Phe 3, Ile 4, and Phe 5, that would remove all of the bulky hydrophobic residues, had an equivalent phenotype to the Sar1[F5D] mutant (Fig. 5 A). Surprisingly, though, when Phe 3 was mutated to Asp (Sar1[F3D]) leaving the bulky Ile4 and Phe5 residues, Sar1 supported efficient COPII vesicle budding (Fig. 5 A). Thus, Phe3 and Phe5 differ in

function. Given the symmetry of the hydrophobic residues (FIF), this would not be expected if the two Phe residues simply functioned similar to a lipid group (such as the myristoyl group found in Arf) for promoting nonspecific bilayer association. These results favor the interpretation that the hydrophobic patch contains sequence specific information that is necessary for Sar1 activity in COP II mediated budding from ER microsomes.

The hydrophobic motif is not essential for nucleotide association or Sec23/24 promoted GTP-hydrolysis

The Phe5 to Asp substitution in the hydrophobic motif could lead to a loss of guanine nucleotide binding, a defect in interaction with the membrane or membrane-associated receptors (such as the membrane-associated mSec12 GEF), or interference with interaction with the cytosolic Sec23/24 complex. To further explore the function of the hydrophobic motif, we first determined that loss of activity was not due to misfolding of the core-fold of Sar1 because the F5D substitution had no effect on nucleotide binding (Fig. S2 B, available at http://www.jcb.org/cgi/content/full/200106039/DC1). To determine if Sar1[F5D] was responsive to the Sar1-specific Sec23/24 GAP complex, we incubated wild-type Sar1 or the Sar1[F5D] mutant with purified Sec23/24 in the presence of $\alpha[^{32}P]$GTP. In both cases, the Sec23/24 complex stimulated the rate of Sar1 GTP hydrolysis to levels previously observed for wild-type Sar1 (Fig. 5 B) (Aridor et al., 1998). Thus, neither intrinsic GDP/GTP binding nor Sec23/24 stimulated GTP hydrolysis, as can be measured by the above assays, are responsible for the defect in function of Sar1[F5D]. The latter results differ strikingly from the effect of mutation of the $\alpha1'$ helix to the Sar1[AAAA] mutant form (Fig. 2 C), suggesting that the NH_2 terminus contains at least two regions that dictate Sar1 function.

The hydrophobic motif is required for stable recruitment of Sar1 to ER membranes

To determine if the hydrophobic motif was involved in Sar1 recruitment to ER membranes, we incubated purified wild-type Sar1 and the Sar1[F5D] mutant with ER microsomes in the presence of GDP, GTP, or GTPγS. Membranes were then pelleted by centrifugation, and membrane and soluble fractions were separated by SDS-PAGE, immunoblotted, and quantitated for Sar1. Very little binding of wild-type Sar1 or the F5D mutant to ER membranes occurs on ice (Aridor et al., 1995; Aridor and Balch, 2000) (Fig. 6 A), indicating the need for physiological activation of Sar1 by the ER-localized Sar1-specific mSec12 GEF. Upon incubation at 32°C, >50% of total wild-type Sar1 added to the assay was stably recruited to membranes in the presence of GTPγS (Fig. 6 A). In contrast, recruitment was not observed with the Sar1[F5D] mutant as <5–10% of Sar1[F5D] was bound under the same conditions (Fig. 6 A).

To determine whether loss of stable membrane association by Sar1[F5D] was not simply due to the absence of Sec23/24 in the binding assay, we examined the ability of Sar1 to recruit Sec23/24 to ER microsomes. While wild-type Sar1 was able

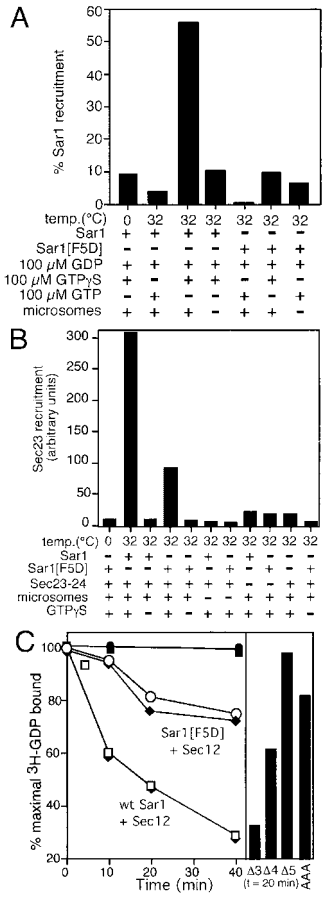

Figure 6. **Sar1[F5D] is defective in stable membrane recruitment and recognition of mSec12.** (A and B) Microsomes were incubated on ice or at 32°C in the presence of ATP (lanes 1–10) or no ATP (lane 11), and either 1 μg Sar1, 1 μg Sar1[F5D], 1 μg Sec23–24, or 100 μM GTP or GTPγS as indicated. Microsomes were then pelleted. The supernatant and pellet were analyzed by SDS-PAGE, immunoblotted, and quantitated for Sar1 (A) or Sec23 (B) (see supplemental Materials and methods, available at http://www.jcb.org/cgi/content/full/200106039/DC1). (C) Exchange activity of Sec12 on wild-type (wt) and mutant Sar1[F5D]. Exchange was measured by preloading Sar1 with [^{3}H]GDP and incubating in the presence of 1 mM cold GTP and the absence or presence of mammalian Sec12 protein (2 μg) as described (Weissman et al., 2001), and the amount of [^{3}H]GDP remaining bound to Sar1 quantitated as described (Nuoffer et al., 1994) (see supplemental Materials and methods, available at http://www.jcb.org/cgi/content/full/200106039/DC1). Closed circles and squares correspond to incubations (2 μg) lacking mSec12 in the presence of Sar1[F5D] or wild-type Sar1, respectively. Closed triangles and diamonds correspond to the level of exchange obtained with wild-type Sar1 or the Sar1[F5D] mutant, respectively, in the absence of detergent.

to efficiently recruit Sec23/24 in the presence of GTP or GTPγS, as shown previously (Aridor et al., 1995, 1998) (Fig. 6 B), incubation of ER microsomes with the Sar1[F5D] mutant in the presence of Sec3/24 and GTP or GTPγS only weakly recruited Sec23/24 (Fig. 6 B). Given that the Sar1[F5D] mutant is not defective in its interaction with the Sec23/24 (Fig. 5 B), it is apparent that the hydrophobic motif facilitates stable recruitment of both Sar1 and Sec23/24 to ER membranes, and that recruitment of Sar1 through the hydrophobic motif precedes stable recruitment of Sec23/24.

The hydrophobic motif facilitates Sar1 activation by the mSec12 exchange factor

Given the inability of the Sar1[F5D] mutant to stably bind membranes (Fig. 6 A) even though interaction with Sec23/24 was normal (Fig. 5 C), we examined the effect of the [F5D] substitution on activation by purified mSec12 GEF in the presence of detergent (Weissman et al., 2001). In contrast to the ability of mSec12 to promote efficient exchange on wild-type Sar1, the Sar1[F5D] mutant was significantly reduced (75% or three- to fourfold) in its rate of exchange in Sec12 GEF stimulated nucleotide exchange (Fig. 6 C). Strikingly, the Δ5-Sar1 truncation completely lost its ability to interact with Sec12 (Fig. 6 C, right panel).

Although the sequence specificity of the FIF motif in COPII vesicle formation suggests that it may be a targeting motif (Fig. 5 A), it remained possible that the FIF sequence could simply promote partitioning of Sar1 into a detergent micelle containing mSec12 in the exchange assay, thereby facilitating efficient exchange. To address this concern, we generated a detergent-free preparation of mSec12 and analyzed the ability of mSec12 to promote exchange in the absence of lipid or detergent. In a detergent-free exchange reaction, we observed no loss of activity of mSec12 in promoting efficient exchange from wild-type Sar1 (Fig. 6 C). Importantly, the inability of the [F5D] mutant to support exchange was identical to the level observed in the presence of detergent (Fig. 6 C). The importance of the NH2-terminal region for Sar1 activation by Sec12 was further demonstrated by generation of Δ25-Sar1, a truncation mutant lacking the entire NH_2 terminus, including the α1′ helix (equivalent to Arf1 [Δ17]). As expected, this truncation has lost its ability to interact with Sec12 (Fig. S4, available at http://www.jcb.org/cgi/content/full/200106039/DC1). Thus, Sar1 requires a conserved hydrophobic motif found in the NH_2 terminus to provide a domain that facilitates activation by the ER-associated mSec12. Given these results, we now refer to this short cluster of bulky hydrophobic amino acids as the STAR motif reflecting its role as a Sar1–NH_2-terminal activation recruitment sequence.

Discussion

We have established a structural foundation for the first committed step in COPII vesicle formation based on the 1.7 Å resolution structure of Sar1. Initiation of vesicle budding involves activation of Sar1, a step that requires a conserved patch of bulky hydrophobic residues found at the NH_2 terminus, the STAR motif, by the Sar1-specific exchange factor mSec12. The hydrophobic motif is unique among modifications of the Ras superfamily GTPases that are used to promote membrane association. Subsequent interactions through a conserved α1′ helix promote stable membrane recruitment. These results lead us to propose that the STAR motif and the α1′ helix confer information that coordinates cargo selection with coat assembly and vesicle budding from the ER for the Sar1 family of GTPases.

The STAR motif is required for recruitment and activation by mSec12

The STAR motif is unique to the Sar1 family and is absent from all other Ras superfamily GTPases including Ras, Rho/Rac/Cdc42, Rab, or Arf family members that utilize generic lipid groups to promote membrane association. One possible role of the NH_2-terminal STAR motif could be similar to that proposed for the Arf1 myristoyl group based on studies with artifical liposomes to facilitate the initial interaction of Arf1 with the lipid bilayer in the GDP-bound state (Antonny et al., 1997; Beraud-Dufour et al., 1999). Although we cannot exclude a partial contribution of the STAR motif to bilayer association, our results favor a more physiological and specific role of STAR motif in Sar1 recruitment given the importance of protein–protein interactions observed in the present study. In particular, whereas substitution of an Asp residue at Phe 3 did not disrupt function in vesicle budding, substitution at the Phe 5 position did, indicating the need for sequence specific information in the motif. These results make it unlikely that the presence of the bulky hydrophobic residues simply confers a generic lipid-like function as observed in Arf. Importantly, measurement of exchange using isolated full-length mSec12 established that the STAR motif facilitates the recognition of mSec12 GEF in an as yet unknown manner. Moreover, mSec12 must be active for recruitment to ER membranes, as Sar1 binding is not observed on ice. Thus, unlike a truncated form of Arf1 (Arf1[Δ17]) in which activation by a soluble, truncated form of ARNO in the absence of lipid or detergent is independent of the myristoyl group and the α1′ helix (Paris et al., 1997; Beraud-Dufour et al., 1998, 1999), Sar1 utilizes STAR motif for interaction with mSec12 and this interaction can facilitate specific membrane recruitment to the ER. One possibility is that the interaction with Sec12 occurs directly through the STAR motif; alternatively, the interaction may be indirect as a result of the effect of the STAR motif on the function or orientation of switch regions I and II. The requirement for the STAR motif in recognition of Sec12 is consistent with the requirement for the STAR motif for inhibition of COPII vesicle budding by the dominant negative Sar1[T39N] mutant in vivo and in vitro, and the essential requirement for the STAR motif in Sar1[T39N] competitive inhibition of microsome-associated mSec12 mediated nucleotide exchange from wild-type Sar1 (Weissman et al., 2001).

We found that the biochemical role of the STAR motif in the initial step in ER membrane recruitment of Sar1 can be observed morphologically. Recently, we have shown that incubation of semiintact cells with Sar1 in the absence of Sec23/24 or Sec13/31 results in the formation of sorting intermediates that take the form of striking, elongated transitional tubules (Aridor et al., 2001). These tubules are precursors to the formation of COPII carriers, as addition of Sec23/24 and Sec13/31 resolves the tubules into carrier vesicles. Consistent with the inability of the [F5D] mutant to engage mSec12, tubule formation does not occur in the presence the Sar1[F5D] mutant (Fig. S3, available at http://www.jcb.org/cgi/content/full/200106039/DC1). Thus, the first detectable event reflecting physiological recruitment of Sar1 to the ER is defective in the absence of a functional STAR motif.

Interaction of Sar1 on ER membranes with Sec23/24

In addition to the information provided by the STAR motif, we found that the α1′ helix is essential for Sar1 function. The Arf1 NH_2-terminal α1′ helix is currently thought to

function in concert with the myristoyl group in promoting the transient partitioning of Arf1-GDP into the bilayer of liposomes (Antonny et al., 1997; Beraud-Dufour et al., 1999). This weak association is stabilized through an unusual β sheet register shift reflecting GTP-dependent conformational changes in switch I and II after activation by Arf1 GEF that displace the α1′ helix from the surface of Arf1 (Goldberg, 1998).

In contrast to the role of the Arf1 α1′ helix in promoting association with the bilayer, we found that the interaction of the Sar1[AAAA] mutant with the ER-associated mSec12 GEF was identical to wild-type Sar1, suggesting that this is not the step in COPII vesicle formation that the α1′ helix is involved. These results support the observation that the [AAAA] substitution does not effect the structural core of Sar1 involved in nucleotide binding, and suggest that it does not interfere with function of switch regions I and II that are involved in recognition of Sec12 (unpublished data). Instead, we found that the Sar1[AAAA] mutant failed to interact with the Sec23/24 coat complex. Given the importance of recruitment of Sec23/24 in building a vesicle coat (Springer et al., 1999) as well as stabilizing the recruitment of Sar1 to ER membranes to promote formation of prebudding complexes (Aridor et al., 1998), these data raise the possibility that formation of the cargo containing prebudding complexes is dependent on the ability of the α1′ helix to direct interaction with Sec23/24.

Structural role of the NH_2-terminal region of Sar1 in COPII vesicle formation

Interaction with GEFs and GAPs by Ras superfamily GTPases normally occurs through switch I and II domains. An important question is how the α1′ helix and STAR motifs structurally contribute to the sequence of events leading to COPII vesicle formation.

In the Arf1-GDP structure, the myristoyl group is thought to be associated with a hydrophobic region on the surface of Arf1 that is opposite to that of the switch elements I and II involved in GEF interaction (Goldberg, 1998). The distinctive orientation of the α1′ helix in Sar1 makes this orientation for the STAR motif unlikely and therefore suggests a different role in COPII vesicle assembly. One possibility is that the NH_2 terminus extending from the Sar1 α1′ helix occupies a site adjacent to switch I in the GDP-bound state (Fig. 7). Indeed, a major structural difference between Arf1 and Sar1 is the lack of an extra β strand, β2ϵ, adjacent to switch I in Arf1 (Amor et al., 1994; Greasley et al., 1995). The β2ϵ strand has been proposed to play an important role in the structural transition from the GDP to GTP states in Arf1 (Antonny et al., 1997; Goldberg, 1998; Beraud-Dufour et al., 1999). Placement of the NH_2 terminus of Sar1 adjacent to switch I could facilitate, either directly or indirectly (as part of a docking platform), recognition of Sec12 through the STAR motif, a configuration consistent with the biochemical data. In this interpretation, the NH_2 terminus could be considered as an additional switch region (III) that serves as a sensor to monitor the activity of soluble and membrane-bound states of Sar1.

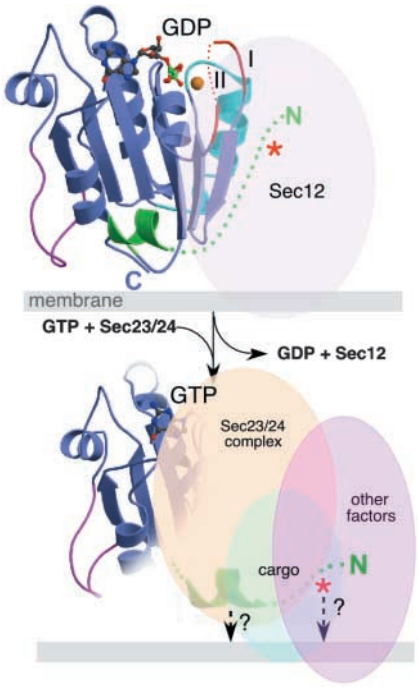

Figure 7. **Model for role of the STAR motif in Sar1 function.** Illustrated is the potential role of the α1′ helix and the STAR motif with ER membranes to promote COPII vesicle formation. In step 1 (top panel), Sar1 is recruited to the ER membrane through participation of the STAR motif in recognition of mSec12. After exchange of GDP for GTP to generate the activated form, in step 2 (bottom panel) Sar1 engages a larger membrane-stable, prebudding complex that includes the Sec23/24 cytosolic component and cargo, defining the selection step in ER export (Kappeler et al., 1997; Aridor et al., 1998, 2001).

The overall structural fold and topological organization of Sar1, although different than Arf, is more homologous to Arf family GTPases than it is to other Ras superfamily GTPases. Such new structural insights lead us to propose that Sar1 and Arf1 form a specialized subgroup of GTPases involved vesicle budding, each with highly specialized function and potentially distinctive modes of interaction with downstream effectors. By analogy to the unusual β sheet register shift in Arf1 during GTP binding that displaces the α1′ helix, activation of Sar1 leading to conformational changes in switch I and II may also displace the NH_2 terminus up to and including the α1′ helix from the surface of Sar1, thereby releasing the α1′ helix residues that facilitate interaction with Sec23/24, as suggested by the current studies (Fig. 7). This model is consistent with our ability to detect only the activated form of Sar1 in stable, detergent insoluble, prebudding protein complexes containing both cargo and the Sec23/24 coat component (Aridor et al., 1998; Kuehn et al., 1998). As it is this step which is likely to define the key event in cargo selection for ER export (Aridor et al., 1998), we suggest that STAR motif based targeting of Sar1 to the ER through mSec12 mediates the ability of the GTPase to specifically coordinate Sec23/24 recruitment with biosynthetic cargo selection at ER export sites (Aridor and Balch, 1996; Aridor et al., 1998, 1999, 2001).

Materials and methods

Structure determination and model refinement

A molecular replacement solution (Navaza, 1994) was obtained using the Arf1-GDP structure (Greasley et al., 1995) as the initial model. These molecular replacement phases did not yield interpretable electron density maps to revewal critical regions of Sar1-GDP structure, but were sufficient to identify 8 out of total 12 selenium sites in the MAD data by cross-phasing using PHASES (Furey and Swaminathan, 1996) with the selenomethionine-Sar1-GDP data ($\lambda = 1.08$ Å) as the native dataset (Tables I and II). These selenium sites were then refined by PHASES and SHARP (De La Fortelle and Bricogne, 1996) programs, and final MAD (Hendrickson, 1991) phases were calculated by SHARP to 1.8 Å with a figure of merit of 0.47. The solvent-flattened MAD electron density map by SOLOMON (Abrahams and Leslie, 1996) was of excellent quality and enabled a model to be refined against the 1.7-Å dataset of wild-type Sar1-GDP crystal using the slowcool annealing and conjugate gradient minimization protocols implemented in CNS version 0.4 (Brunger et al., 1998). The high quality of the MAD data allowed refinement to converge quickly to an R_{cryst} of 0.22 and an R_{free} of 0.24. Most of the residues (92%) are in most favored regions of the Ramachandran plot (Laskowski et al., 1993), except residues, A47, A84, B48, that are in either disallowed or generously allowed regions of Ramachandran plot (Laskowski et al., 1993). These three residues have poor electron density and are in the flexible switch regions. The coordinates and structure factors have been deposited with the Protein Databank with the ID code 1F6B.

Online supplemental material

Online supplemental Fig. 1 shows the structural organization of Sar1 and ARF1. Online supplemental Fig. 2 shows ths nucleotide binding assay. Online supplemental Fig. 3. shows that the Sar1[F5D] mutant cannot support tubule formation in vitro. Online supplemental Fig. 4 shows that Δ25-Sar1 is defective in recognition of Sec12. Supplemental material is available at http://www.jcb.org/cgi/content/full/200106039/DC1.

We thank the staff at Stanford Synchrotron Radiation Laboratory (Menlo Park, CA), beamlines 7-1 and 9-2 for excellent assistance in data collection.

This work was supported by National Institutes of Health grants GM42336 (W.E. Balch) and GM49497 (I.A. Wilson). S. Béraud-Dufour was supported by a fellowship from La Ligue Nationale Contre le Cancer and Human Frontiers in Science Fellowship.

Submitted: 7 June 2001
Revised: 17 October 2001
Accepted: 17 October 2001

References

Abrahams, J.P., and G.W. Leslie. 1996. *SOLOMON. Acta Crystallogr.* D52:30–42.

Amor, J.C., D.H. Harrison, R.A. Kahn, and D. Ringe. 1994. Structure of the human ADP-ribosylation factor 1 complexed with GDP. *Nature.* 372:704–708.

Antonny, B., S. Beraud-Dufour, P. Chardin, and M. Chabre. 1997. N-terminal hydrophobic residues of the G-protein ADP-ribosylation factor-1 insert into membrane phospholipids upon GDP to GTP exchange. *Biochemistry.* 36: 4675–4684.

Aridor, M., and W.E. Balch. 1996. Principles of selective transport: coat complexes hold the key. *Trends Cell Biol.* 6:315–320.

Aridor, M., and W.E. Balch. 2000. Kinase signaling initiates COPII recruitment and export from the mammalian endoplasmic reticulum. *J. Biol. Chem.* 275: 35673–35676.

Aridor, M., S.I. Bannykh, T. Rowe, and W.E. Balch. 1995. Sequential coupling between COPII and COPI vesicle coats in endoplasmic reticulum to Golgi transport. *J. Cell Biol.* 131:875–893.

Aridor, M., J. Weissman, S. Bannykh, C. Nouffer, and W.E. Balch. 1998. Cargo selection by the COPII budding machinery during export from the endoplasmic reticulum. *J. Cell Biol.* 141:61–70.

Aridor, M., S.I. Bannykh, T. Rowe, and W.E. Balch. 1999. Cargo can modulate the formation of COPII coated vesicles. *J. Biol. Chem.* 274:4389–4399.

Aridor, M., K.N. Fish, S. Bannykh, J. Weissman, T.H. Roberts, J. Lippincott-Schwartz, and W.E. Balch. 2001. The Sar1 GTPase coordinates biosynthetic cargo selection with endoplasmic reticulum export site assembly. *J. Cell Biol.* 152:213–229.

Balch, W.E., J.M. McCaffery, H. Plutner, and M.G. Farquhar. 1994. Vesicular stomatitis virus glycoprotein is sorted and concentrated during export from the endoplasmic reticulum. *Cell.* 76:841–852.

Barlowe, C. 1998. COPII and selective export from the endoplasmic reticulum. *Biochim. Biophys. Acta.* 1404:67–76.

Barlowe, C., C. d'Enfert, and R. Schekman. 1993. Purification and characterization of SAR1p, a small GTP-binding protein required for transport vesicle formation from the endoplasmic reticulum. *J. Biol. Chem.* 268:873–879.

Barlowe, C., L. Orci, T. Yeung, M. Hosobuchi, S. Hamamoto, N. Salama, M.F. Rexach, M. Ravazzola, M. Amherdt, and R. Schekman. 1994. COPII: a membrane coat formed by Sec proteins that drive vesicle budding from the endoplasmic reticulum. *Cell.* 77:895–907.

Beraud-Dufour, S., S. Paris, M. Chabre, and B. Antonny. 1999. Dual interaction of ADP ribosylation factor 1 with Sec7 domain and with lipid membranes during catalysis of guanine nucleotide exchange. *J. Biol. Chem.* 274:37629–37636.

Beraud-Dufour, S., S. Robineau, P. Chardin, S. Paris, M. Chabre, J. Cherfils, and B. Antonny. 1998. A glutamic finger in the guanine nucleotide exchange factor ARNO displaces Mg2+ and the beta-phosphate to destabilize GDP on ARF1. *EMBO J.* 17:3651–3659.

Brunger, A.T., P.D. Adams, G.M. Clore, W.L. DeLano, P. Gros, R.W. Grosse-Kunstleve, J.S. Jiang, J. Kuszewski, M. Nilges, N.S. Pannu, et al. 1998. Crystallography & NMR system: a new software suite for macromolecular structure determination. *Acta Crystallogr.* D54:905–921.

D'Enfert, C., C. Barlowe, S.-I. Nishikawa, A. Nakano, and R. Schekman. 1991. Structural and functional dissection of a membrane glycoprotein required for vesicle budding from the endoplasmic reticulum. *Mol. Cell. Biol.* 11: 5727–5734.

De La Fortelle, E., and G. Bricogne. 1996. *Sharp. Meth. Enzymol.* 276:472–494.

Furey, W., and S. Swaminathan. 1996. *PHASES. Meth. Enzymol.* 276:277.

Goldberg, J. 1998. Structural basis for activation of ARF GTPase: mechanisms of guanine nucleotide exchange and GTP-myristoyl switching. *Cell.* 95:237–248.

Greasley, S.E., H. Jhoti, C. Teahan, R. Solari, A. Fensome, G.M. Thomas, S. Cockcroft, and B. Bax. 1995. The structure of rat ADP-ribosylation factor-1 (ARF-1) complexed to GDP determined from two different crystal forms. *Nat. Struct. Biol.* 2:797–806.

Hendrickson, W.A. 1991. Determination of macromolecular structures from anomalous diffraction of synchrotron radiation. *Science.* 254:51–58.

Hicke, L., and R. Schekman. 1989. Yeast Sec23p acts in the cytoplasm to promote protein transport from the endoplasmic reticulum to the Golgi complex in vivo and in vitro. *EMBO J.* 8:1677–1684.

Hillig, R.C., M. Hanzal-Bayer, M. Linari, J. Becker, A. Wittinghofer, and L. Renault. 2000. Structural and biochemical properties show ARL3-GDP as a distinct GTP binding protein. *Structure Fold Des.* 8:1239–1245.

Jackson, C.L., and J.E. Casanova. 2000. Turning on ARF: the Sec7 family of guanine-nucleotide-exchange factors. *Trends Cell Biol.* 10:60–67.

Jones, D.H., B. Bax, A. Fensome, and S. Cockcroft. 1999. ADP ribosylation factor 1 mutants identify a phospholipase D effector region and reveal that phospholipase D participates in lysosmal secretion but is not sufficient for recruitment of coatomer 1. *Biochem. J.* 341:185–192.

Kahn, R.A., C. Goddard, and M. Newkirk. 1988. Chemical and immunological characterization of the 21-kDa ADP- ribosylation factor of adenylate cyclase. *J. Biol. Chem.* 263:8282–8287.

Kappeler, F., D.R. Klopfenstein, M. Foguet, J.P. Paccaud, and H.P. Hauri. 1997. The recycling of ERGIC-53 in the early secretory pathway. ERGIC-53 carries a cytosolic endoplasmic reticulum-exit determinant interacting with COPII. *J. Biol. Chem.* 272:31801–31808.

Kraulis, P.J. 1991. MOLSCRIPT: a program to produce both detailed and schematic plots of protein structure. *J. Appl. Crystallgr.* 24:946–950.

Kuehn, M.J., M. Herrmann, and R. Schekman. 1998. COPII-cargo interactions direct protein sorting into ER-derived transport vesicles. *Nature.* 391:187–190.

Kuge, O., C. Dascher, L. Orci, T. Rowe, M. Amherdt, H. Plutner, M. Ravazzola, G. Tanigawa, J.E. Rothman, and W.E. Balch. 1994. Sar1 promotes vesicle budding from the endoplasmic reticulum but not Golgi compartments. *J. Cell Biol.* 125:51–65.

Laskowski, R.A., M.W. MacArthur, S.D. Moss, and J.M. Thornton. 1993. PROCHECK: a program to check the stereochemical quality of protein structures. *J. Appl. Crystallogr.* 26:283–291.

Menetrey, J., E. Macia, S. Pasqualato, M. Franco, and J. Cherfils. 2000. Structure

of Arf6-GDP suggests a basis for guanine nucleotide exchange factors specificity. *Nat. Struct. Biol.* 7:466–469.

Merritt, E.A., S. Sarfaty, I.K. Feil, and W.G. Hol. 1997. Structural foundation for the design of receptor antagonists targeting Escherichia coli heat-labile enterotoxin. *Structure.* 5:1485–1499.

Nakano, A., and M. Muramatsu. 1989. A novel GTP-binding protein, Sar1p, is involved in transport from the endoplasmic reticulum to the Golgi apparatus. *J. Cell Biol.* 109:2677–2691.

Nakano, A., D. Brada, and R. Schekman. 1988. A membrane glycoprotein, Sec12p, required for protein transport from the endoplasmic reticulum to the Golgi apparatus in yeast. *J. Cell Biol.* 107:851–863.

Navaza, J. 1994. AMoRe: an automated package for molecular replacement. *Acta Crystallogr.* A50:157–163.

Nuoffer, C.N., H.W. Davidson, J. Matteson, J. Meinkoth, and W.E. Balch. 1994. A GDP-bound form of Rab1 inhibits protein export from the endoplasmic reticulum and transport between Golgi compartments. *J. Cell Biol.* 125: 225–237.

Palade, G.E. 1975. Intracellular aspects of the process of protein transport. *Science.* 189:347–354.

Paris, S., S. Beraud-Dufour, S. Robineau, J. Bigay, B. Antonny, M. Chabre, and P. Chardin. 1997. Role of protein-phospholipid interactions in the activation of ARF1 by the guanine nucleotide exchange factor Arno. *J. Biol. Chem.* 272:22221–22226.

Rowe, T., and W.E. Balch. 1995. Expression and purification of mammalian Sar1. Methods in Enzymology, ed W.E. Balch, C.J. Der and A. Hall. Small GTPases and their regulators: part C. *Proteins involved in transport.* 257: 49–53.

Rowe, T., M. Aridor, J.M. McCaffery, H. Plutner, and W.E. Balch. 1996. COPII vesicles derived from mammalian endoplasmic reticulum (ER) microsomes recruit COPI. *J. Cell Biol.* 135:895–911.

Saito, Y., K. Kimura, T. Oka, and A. Nakano. 1998. Activities of mutant Sar1 proteins in guanine nucleotide binding, GTP hydrolysis, and cell-free transport from the endoplasmic reticulum to the Golgi apparatus. *J. Biochem.* 124: 816–823.

Schweins, T., and A. Wittinghofer. 1994. GTP-binding proteins. Structures, interactions and relationships. *Curr. Biol.* 4:547–550.

Seabra, M.C. 1998. Membrane association and targeting of prenylated Ras-like GTPases. *Cell Signal.* 10:167–172.

Springer, S., A. Spang, and R. Schekman. 1999. A primer on vesicle budding. *Cell.* 97:145–148.

Vetter, I.R., and A. Wittinghofer. 2001. The guanine nucleotide-binding switch in three dimensions. *Science.* 294:1299–1304.

Weissman, J., H. Plutner, and W.E. Balch. 2001. The mammalian Sar1 exchange factor mSec12 is essential for endoplasmic reticulum export. *Traffic.* 2:465–475.

Wieland, F., and C. Harter. 1999. Mechanisms of vesicle formation: insights from the COP system. *Curr. Opin. Cell Biol.* 11:440–446.

Wittinghofer, A., and E.F. Pai. 1991. The structure of Ras protein: a model for a universal molecular switch. *Trends Biochem. Sci.* 16:382–387.

Yoshihisa, T., C. Barlowe, and R. Schekman. 1993. Requirement for a GTPase-activating protein in vesicle budding from the endoplasmic reticulum. *Nature.* 259:1466–1468.